Author(s): Lehtinen, P. O. & Foster, A. S. & Ayuela, A. & Vehviläinen, T. T. & Nieminen, Risto M.

Title: Structure and magnetic properties of adatoms on carbon nanotubes

Year: 2004

Version: Final published version

Please cite the original version:

Lehtinen, P. O. & Foster, A. S. & Ayuela, A. & Vehviläinen, T. T. & Nieminen, Risto M. 2004. Structure and magnetic properties of adatoms on carbon nanotubes. Physical Review B. Volume 69, Issue 15. 155422/1-5. ISSN 1550-235X (electronic). DOI: 10.1103/physrevb.69.155422.

Structure and magnetic properties of adatoms on carbon nanotubes

P. O. Lehtinen,[1] A. S. Foster,[1] A. Ayuela,[2] T. T. Vehviläinen,[1] and R. M. Nieminen[1]
[1]*Laboratory of Physics, Helsinki University of Technology, P.O. Box 1100, 02015, Finland*
[2]*Donostia International Physics Center (DIPC), P.O. Box 1072, 20018 San Sebastian, Donostia, Spain*
(Received 27 October 2003; published 20 April 2004)

We use *ab initio* methods to calculate the physical and electronic properties of carbon adatoms on different characteristic carbon nanotubes. We found that for every tube the energetically favored adsorption geometry is a ''bridgelike'' structure between two surface carbons, perpendicular to the long axis of the tube. For adsorption perpendicular or parallel to the axis, the calculations show that the adatom is spin polarized, although the magnitude of the magnetic moment depends mainly on the electronic structure of the nanotube itself.

DOI: 10.1103/PhysRevB.69.155422 PACS number(s): 73.22.−f, 75.75.+a, 73.20.Hb

I. INTRODUCTION

As the focus in nanotube studies becomes increasingly atomistic, the importance of defects in nanotube properties is more frequently highlighted. Understanding the properties of these defects has become an essential part of such diverse processes in carbon materials such as strain,[1] lithium storage in nanotube based batteries,[2] catalytic growth,[3] junctions,[4] and quantum dot creation.[5,6] Studies of radiation effects[7] in graphite and other carbon nanostructures and experiments on as-grown nanotubes[5,8] have demonstrated that intrinsic carbon defects are a common phenomenon in standard samples. One of the most common intrinsic defects created is the carbon vacancy-adatom pair,[7] and therefore it is important to study the influence this kind of defect will have on the surface physical and electronic structure. Recently, this defect pair has been considered on graphite,[9] and the adatom on graphene,[10] so here we expand the study to nanotubes.

The study of intrinsic defects in pure carbon systems has also become of specific interest currently due to the recent experimental demonstrations of magnetism in pure carbon systems.[11–15] Some of these studies have speculated that intrinsic carbon defects could be responsible for the observed magnetic properties.[11] Some theoretical studies have predicted magnetism in defective fullerenes,[16,17] and we have demonstrated previously that an adatom on a graphene sheet is magnetic,[10] hence it is also important to see if this behavior is consistent for nanotubes.

In order to make the following discussion transparent, at this point we will introduce some fundamental concepts in carbon and carbon nanotube physics. The carbon atom has four valence electrons, and in graphite carbons are ordered in such a way that they form a net of hexagons where every carbon atom has three nearest neighbors. This means that three out of four electrons form sp^2 bonds in the graphite plane. The remaining p orbital is perpendicular to the surface and forms metallic π bands across the surface. The interaction between layers is of weak, van der Waals type.

A nanotube can be considered as a rolled graphene sheet (a single plane of graphite). The nature of the rolling decides many of the tube's electronic properties and this is indicated by the so-called chiral vector—given as (n,m). If the nanotube's chiral vector is of the form $(n,0)$ the nanotube is called zigzag. If the chiral vector has form (n,n) then the tube is called armchair. The rest of the tubes are called chiral nanotubes. The determination of whether a tube is a metallic or semiconducting is as follows: if $n-m$ is divisible by 3 the tube is metallic, otherwise it is semiconducting. This can be understood in terms of zone folding and analogy to graphite—the degenerate $\pi\pi^*$ bands at the K point of the graphite Brillouin zone are folded into the Γ point in the nanotube.[18–21] However, this type of description does not take into account the effect of curvature. Due to the curvature of the nanotube the π^* and σ^* bonds hybridize and thus a small gap opens in zigzag nanotubes. This effect is strongest with nanotubes which have radius less than that of C_{60}.[22] Table I shows the effective ''class'' of the nanotubes used in this study according to this analysis.

II. METHODS

The calculations have been performed using the plane-wave basis VASP code,[23,24] implementing the spin-polarized density-functional theory (DFT) and the generalized gradient approximation of Perdew and and Wang[25] known as PW91. To represent the core ($1s^2$) electrons of carbon we have used projector augmented wave (PAW) potentials.[26,27] $2s^2$ and $2p^2$ electrons are considered as valence electrons. A kinetic energy cutoff of 400 eV was found to give energy convergence of up to a few meV.

In order to check the validity of the PAW potentials we initially determined the lattice parameters for the bulk graphite. The calculated lattice constants for graphite are $a=2.467$ Å and $c=6.925$ Å using a Monkhorst-Pack[28] $8\times8\times8k$-point grid to sample the Brillouin zone. The experimental values are 2.464 Å and 6.711 Å (Ref. 29) for a and c, respectively. The calculated a is thus only 0.1% larger than the experimental while the difference in the interlayer distance is 3.2%. Note that the agreement in c is fortuitious, since DFT does not reproduce the real interlayer van der Waals interactions.[30] However, as long as we avoid interlayer processes our method should provide a very good model for these carbon systems.

For each tube considered we checked the dependence of the results on k-point sampling and the vacuum surrounding the tube. Generally a k-point mesh of $(1\times1\times7)$ (Γ point included) and a vacuum gap of about 9 Å was enough to converge the total energy of the system to within 10 meV. Since we are considering defects in this study, it was also important to check the influence of defect-defect interactions

TABLE I. Data for the various nanotubes considered in this study. The values for a graphene sheet are given as in Ref. 10.

Nanotube	Class	Radius (Å)	Adsorption energy (eV)		Magnetic moment (μ_B)	
			Parallel	Perpendicular	Parallel	Perpendicular
(8,0)	Semiconducting	3.13	2.37	2.89	0.01	0.23
(10,0)	Semiconducting	3.96	2.09	2.57	0.25	0.23
(11,0)	Semiconducting	4.41	2.03	2.49	0.20	0.22
(5,5)	Metallic	3.39	2.33	3.29	0.23	0.44
(9,0)	Semiconducting	3.57	2.35	2.80	0.24	0.35
(6,6)	Metallic	4.07	2.15	2.91	0.27	0.43
(12,0)	Semiconducting	4.97	2.04	2.50	0.32	0.36
Graphene	Metallic	∞	1.40	1.40	0.45	0.45

along the tube (radially they are suppressed by the vacuum). We found that a nanotube length providing three carbon rings gave a good model of isolated adatom defects on the tube surface. Figures 1 and 2 show examples of the defected unit cells used for (5,5) and (9,0) nanotubes. The (5,5), (6,6), (8,0), (9,0), (10,0), (11,0), and (12,0) nanotubes used unit cells containing $60+1$, $72+1$, $64+1$, $72+1$, $80+1$, $88+1$, and $96+1$ atoms, respectively.

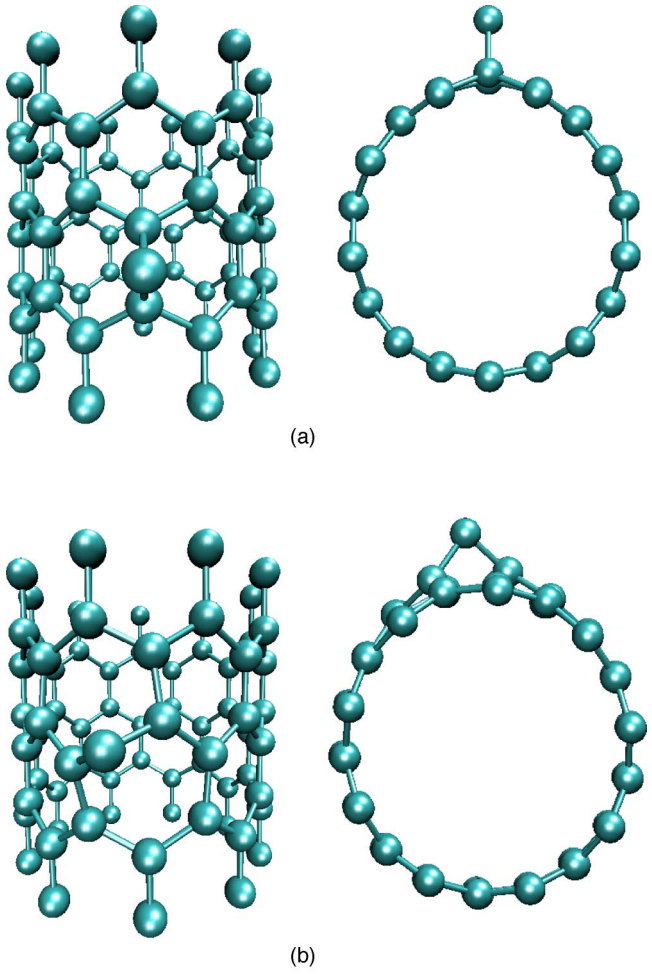

FIG. 1. The equilibrium positions of an adatom on a (9,0) nanotube in the (a) parallel and (b) perpendicular positions.

III. RESULTS

A. Physical structure

In this study we consider seven nanotubes: the (8,0), (9,0), (10,0), (11,0), (12,0), (5,5), and (6,6) tubes. These nanotubes provide a reasonable sample of nanotube radius, chirality and electronic structure. Table I summarizes the properties of the various nanotubes. By the rule discussed previously, the (8,0), (10,0), and (11,0) are semiconducting, and (5,5) and (6,6) are metallic. (9,0) and (12,0) are formally metallic, but due to their radius a small band gap opens.

For each tube the qualitative behavior of adatoms on the surface is very similar—the adatom adsorbs in a bridgelike

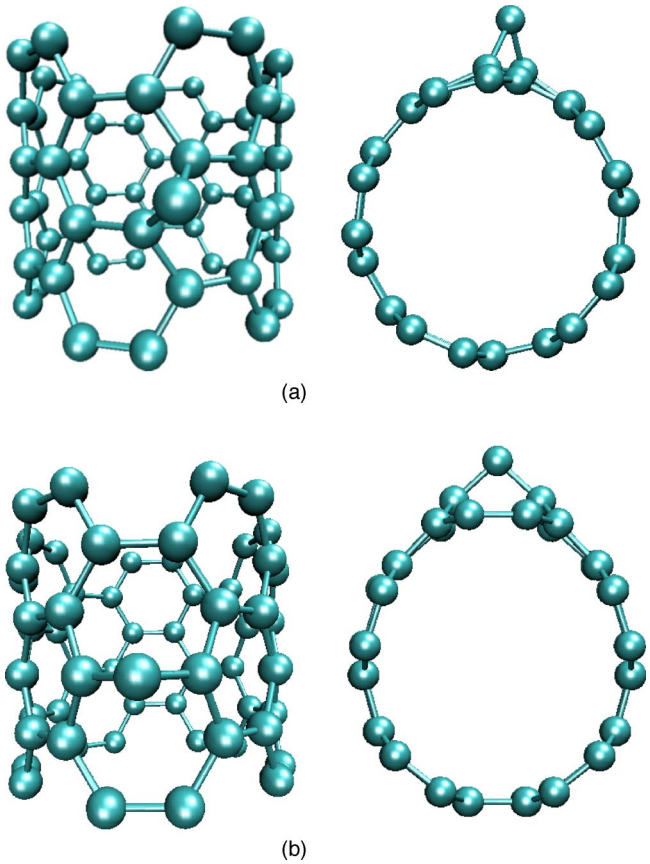

FIG. 2. The equilibrium positions of an adatom on a (5,5) nanotube in the (a) parallel and (b) perpendicular positions.

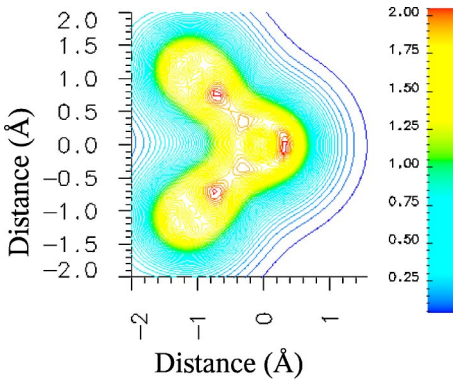

FIG. 3. (Color online) The charge density in a plane of an adatom on (10,0) nanotube at perpendicular position. The view is from the side of the triangle formed by the adatom and the nearest neighbors. The origin corresponds to the position of the adatom.

position between two carbon surface atoms (see, for example, Figs. 1 and 3). This behavior is similar to that seen for previous calculations of adatoms on a graphene sheet.[3,10,31,32] However, for nanotubes the adatom can form a bridge either ''parallel'' (see Fig. 4) or ''perpendicular'' (see Fig. 4) to the tubes' axis. Table I gives the adsorption energies for both positions of each nanotube. This energy was found by subtracting the total energy of an ideal tube and an isolated carbon in the triplet state from the total energy of the defected tube. It is immediately evident that in every case the perpendicular position is the favored site. This can be understood from simple carbon bonding considerations: in the perpendicular case it is easier for the adatom to push the two adjacent nanotube atoms apart, since the curvature increases the distance to neighboring carbons in the perpendicular direction. For tubes of similar electronic structure, the adsorption energy reduces as the radius increases, and this supports the bonding argument. Increasing the radius means the surface atoms are closer together and more difficult to separate—graphene is the limiting case, where the surface atoms are closest, and here we see the smallest adsorption energy. The differences between semiconducting and metallic tubes clearly reflect the difference in electronic structure, with adatoms being more easily adsorbed onto the more weakly bonded metallic tubes in the perpendicular position.

B. Magnetic properties

The model of magnetism for adatoms on a graphene sheet presented previously[10] is based on a simple electron counting argument. Both the two bonded atoms on the surface, as well as the adatom, present a different hybridization: the surface atoms attached to the adatom have a sp^2-sp^3 hybridization while the adatom stays sp^2-like, as seen in the model of Fig. 4. Concerning the adatom, the counting of the four carbon electrons is as follows: two electrons participate in the covalent bond with the graphene carbons. From the two remaining electrons, one goes to the dangling sp^2 bond, and another is shared between the sp^2 bond and the p_z orbital. This p_z orbital is orthogonal to the surface π orbitals and cannot form any bands, remaining localized and therefore spin polarized. Figure 4 shows clearly that the spin polarized density

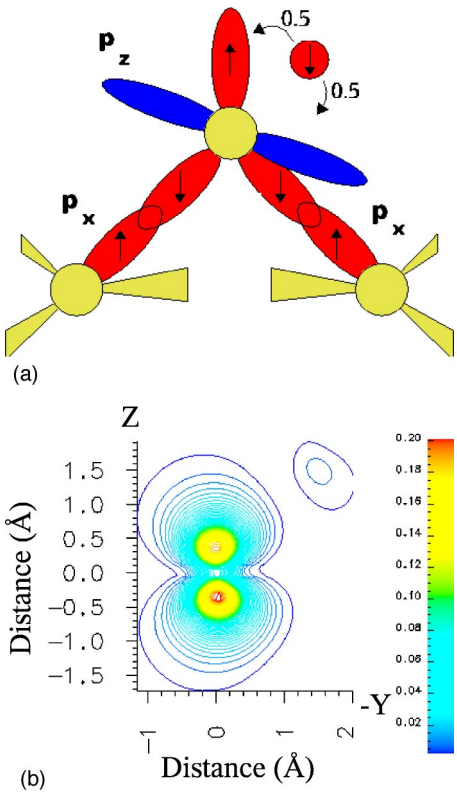

FIG. 4. (Color online) (a) A schematic diagram of the bond orbitals at the equilibrium position in a plane through the adatom and the two surface carbons. Note that this schematic is a projection, and that the p_z orbital is orthogonal to the adatom-surface bonds. (b) The spin density in $e/\text{Å}^3$ of a plane normal to the surface through the center of the adatom when the adatom is at the equilibrium position. The adatom is at (0,0).

occupies p orbitals of the adatom. Recent results on other systems[33–35] demonstrated that this behavior is typical for low-dimensional systems. The half electron of the p_z orbital provides the magnetization of around 0.5 μ_B. In addition the sp^2-sp^3 hybridization of the graphene carbon linked to the adatom decides the adsorption energetics of the adatom. This implies that on nanotubes, where the bonding is similar, adatoms should also be magnetic. Table I shows that for all the nanotubes considered in this study, adsorbed adatoms have a finite magnetic moment. The specific magnitude of the magnetic moment depends, as for the adsorption energies, on the adsorption geometry and electronic structure of the tube as is explained in the following paragraphs.

Geometrically the magnetic moment is influenced by the ability of the polarized p_z orbital to form bands with the surface π orbitals. In graphene the p_z orbital is orthogonal to the π orbitals, and we get the maximum moment of 0.45 μ_B. For adsorption positions on nanotubes which locally correspond to graphene, i.e., the perpendicular sites on (5,5) and (6,6) (see Fig. 2), the magnetic moment is almost equivalent, as shown in Table I. This argument can be extended if we consider graphenelike electronic structure as the limiting configuration, i.e., that it is energetically favorable for nonmetallic nanotubes to become more metallic. For semiconducting tubes the adatom acts as a dopant, and some

of its charge density is delocalized around the system making the nanotube more metallic, and consequently reducing the localized magnetic moment on the adatom. If we apply this argument to the results shown in Table I, we see that it explains the general trends in magnetic moment. The smallest moments are seen for the ''large'' gap semiconducting tubes, (8,0), (10,0), and (11,0) nanotubes. Here, a large portion of the adatom charge is delocalized. Larger moments, and hence less delocalization, are seen for those tubes where the gap is a consequence of the radius of the tube, and therefore smaller [0.13 eV for (9,0) compared to 0.73 eV for (10,0) in our calculations]—this applies to nanotubes (9,0) and (12,0). To support this idea we calculated the density of the states of the ideal and defected (9,0) and (10,0) nanotubes. The (9,0) nanotube with a defect is metallic, i.e., the gap disappears, while (10,0) remains a semiconductor with a reduced band gap.

To understand the differences of magnetic moments of an adatom at parallel and perpendicular adsorption sites, we must consider the interaction of the adatom with itself around the circumference of the tube. The adatom's magnetic orbital causes a perturbation in the local charge density around the defect site, and the magnitude of this perturbation depends on the electronic structure of the tube (it is larger for metallic nanotubes where charge density is less localized). For small nanotube radii, this perturbation can extend beyond half the circumference of the tube, and hence interacts with itself. This self-interaction only occurs when there is a component of the magnetic orbital perpendicular to the tube axis, i.e., it has no effect on the perpendicular adsorption sites of adatom on (5,5) and (6,6) since the magnetic orbitals lie along the tube axis. Combining both the electronic structure and self-interaction effects we can summarize the behavior of the magnetic moments.

(1) For semiconducting tubes (10,0) and (11,0) the electronic structure reduces the moments, but the radii are large enough to avoid self-interaction.

(2) For tubes (5,5) and (6,6) with adatoms in parallel adsorption sites, strong self-interaction reduces the moments.

(3) For (9,0), a combination of small electronic structure effect and self-interaction reduce the moment.

(4) For (12,0) the radius is large enough to avoid self-interaction, and the moment is slightly reduced due to electronic structure.

(5) For (8,0) nanotube adatom in a parallel adsorption site we get both strong electronic structure and self-interaction components resulting in a near zero moment.

The (8,0) nanotube acts as the limiting case for these effects due to its semiconducting nature and very small radius. In the parallel-bridge case the interaction of the adatom with itself is much larger so that the ferromagnetism disappears. In the perpendicular-bridge position, the small radius of the tube is not so important since the magnetic orbital now lies almost along the translational axis of the tube (see Fig. 1). The diameter of the (8,0) nanotube is the limit for magnetic interactions in semiconductor-type tubes. This limit is in agreement and shifted just a little bit from the onset of metallicity problems due to the curvature in the (9,0) tube.

For some adsorption sites on semiconductor nanotubes, the maximum spin-polarization density is along the tube axis (see Fig. 1), while in metallic nanotubes the spin-polarization density is perpendicular to the plane of the adatom and its nearest neighbors. These differences between metallic and semiconductor nanotube coupling with the lattice are interesting, and will influence the Curie temperatures. It seems that the doped semiconductor tubes, both because they show less magnetization as well as a different role of the tube direction, will show lower Curie temperatures.

IV. SUMMARY

In this study we have considered the adsorption of carbon adatoms onto the outside surface of various carbon nanotubes. We found that for every tube the energetically favored adsorption geometry is a ''bridgelike'' structure between two surface carbons, as predicted in previous calculations of a graphene sheet.[10] For all nanotubes a configuration with this bridge perpendicular to the long axis of the tube was preferable. The calculated adsorption energies decrease with increasing radius of the nanotube, tending towards the ''infinite'' radius graphene case.

We have also demonstrated that the magnetic moment previously predicted for adatoms on graphene is also present in calculations of nanotubes. For the wide variety of nanotubes considered, we find that an adatom adsorbed onto the tube is only nonmagnetic (or very weakly magnetic) for the parallel-bridge position on an (8,0) nanotube. In all other cases, the magnetic moment is in the range 0.20–0.44 μ_B, with the specific local bonding configuration of the adatom and the electronic structure of the nanotube determining the magnitude of the magnetic moment. For tubes that are initially semiconducting, we find that the adsorption of an adatom reduces or even removes the band gap due to delocalization of the adatom charge density.

Due to the computational cost of such calculations, we did not consider adatom diffusion explicitly in this study. However, tight-binding simulations for nanotubes[36] have demonstrated that adatoms can be very mobile on nanotube surfaces, with migration barriers close to the graphene limit of 0.5 eV (Ref. 10) for radii as small as 1 nm. This is consistent with experimental observations that many defects on nanotube surfaces can be removed by annealing.[7] Hence, it should be possible to control the concentration, and therefore magnetism, of these defects on nanotubes via temperature. A further consequence of this high mobility is that it would be important to consider the interactions between adatoms, and whether stable carbon clusters could nucleate on the surface. If these clusters exist, it would be very interesting to see whether they also exhibit magnetic properties.

ACKNOWLEDGMENTS

This work was supported by Academy of Finland through its Center of Excellence Program (2000-2005). We are grateful to Center of Scientific Computing, Espoo, for use of its computational resources. The LEV00 code[37] was used for calculating the density maps. We wish to thank A. Krasheninnikov and K. Nordlund for useful discussions.

[1] G.G. Samsonidze, G.G. Samsonidze, and B.I. Yakobson, Phys. Rev. Lett. **88**, 065501 (2002).
[2] V. Meunier, J. Kephart, C. Roland, and J. Bernholc, Phys. Rev. Lett. **88**, 075506 (2002).
[3] Y.H. Lee, S.G. Kim, and D. Tománek, Phys. Rev. Lett. **78**, 2393 (1997).
[4] M. Ouyang, J.L. Huang, C.L. Cheung, and C.M. Lieber, Science **291**, 97 (2001).
[5] M. Bockrath, W.J. Liang, D. Bozovic, J.H. Hafner, C.M. Lieber, M. Tinkham, and H. Park, Science **291**, 283 (2001).
[6] M.T. Woodside and P.L. McEuen, Science **296**, 1098 (2002).
[7] F. Banhart, Rep. Prog. Phys. **62**, 1181 (1999).
[8] T. Maltezopoulos, A. Kubetzka, M. Morgenstern, and R. Wiesendanger, Appl. Phys. Lett. **83**, 1011 (2003).
[9] C.P. Ewels, R.H. Telling, A.A. El-Barbary, M.I. Heggie, and P.R. Briddon, Phys. Rev. Lett. **91**, 025505 (2003).
[10] P.O. Lehtinen, A.S. Foster, A. Ayuela, A. Krasheninnikov, K. Nordlund, and R.M. Nieminen, Phys. Rev. Lett. **91**, 017202 (2003).
[11] T.L. Makarova, B. Sundqvist, R. Höhne, P. Esquinazi, Y. Kopelevich, P. Scharff, V.A. Davydov, L.S. Kashevarova, and A.V. Rakhmanina, Nature (London) **413**, 716 (2001).
[12] S. Bandow, F. Kokai, K. Takahashi, M. Yudasaka, and S. Iijima, Appl. Phys. A: Mater. Sci. Process. **73**, 281 (2001).
[13] P. Esquinazi, A. Setzer, R. Höhne, C. Semmelhack, Y. Kopelevich, D. Spemann, T. Butz, B. Kohlstrunk, and M. Lösche, Phys. Rev. B **66**, 024429 (2002).
[14] R.A. Wood, M.H. Lewis, M.R. Lees, S.M. Bennington, M.G. Cain, and N. Kitamura, J. Phys.: Condens. Matter **14**, L385 (2002).
[15] J.M.D. Coey, M. Venkatesan, C.B. Fitzgerald, A.P. Douvalis, and I.S. Sanders, Nature (London) **420**, 156 (2002).
[16] A.N. Andriotis, M. Menon, R.M. Sheetz, and L. Chernozatonskii, Phys. Rev. Lett. **90**, 026801 (2003).
[17] Y.H. Kim, J. Choi, K.J. Chang, and D. Tománek, Phys. Rev. B **68**, 125420 (2003).
[18] N. Hamada, S.I. Sawada, and A. Oshiyama, Phys. Rev. Lett. **68**, 1579 (1992).
[19] J.W. Mintmire, B.I. Dunlap, and C.T. White, Phys. Rev. Lett. **68**, 631 (1992).
[20] M.S. Dresselhaus, G. Dresselhaus, and R. Saito, Phys. Rev. B **45**, 6234 (1992).
[21] O. Gülseren, T. Yildirim, and S. Ciraci, Phys. Rev. B **65**, 153405 (1992).
[22] R. Saito, G. Dresselhaus, and M. Dresselhaus, *Physical Properties of Carbon Nanotubes* (Imperial College Press, London, 1998).
[23] G. Kresse and J. Furthmüller, Comput. Mater. Sci. **6**, 15 (1996).
[24] G. Kresse and J. Furthmüller, Phys. Rev. B **54**, 11 169 (1996).
[25] J.P. Perdew, J.A. Chevary, S.H. Vosko, K.A. Jackson, M.R. Pederson, D.J. Singh, and C. Fiolhais, Phys. Rev. B **46**, 6671 (1992).
[26] G. Kresse and D. Joubert, Phys. Rev. B **59**, 1758 (1999).
[27] P.E. Blöchl, Phys. Rev. B **50**, 17 953 (1994).
[28] H. Monkhorst and J. Pack, Phys. Rev. B **13**, 5188 (1976).
[29] See M. Winter, *www.webelements.com*, 2001.
[30] E. Hult, P. Hyldgaard, J. Rossmeisl, and B.I. Lundqvist, Phys. Rev. B **64**, 195414 (2001).
[31] K. Nordlund, J. Keinonen, and T. Mattila, Phys. Rev. Lett. **77**, 699 (1996).
[32] M. Heggie, B.R. Eggen, C.P. Ewels, P. Leary, S. Ali, G. Jungnickel, R. Jones, and P.R. Briddon, Proc.-Electrochem. Soc. **6**, 60 (1998).
[33] S. Watanabe, M. Ichimura, T. Onogi, Y.A. Ono, T. Hashizume, and Y. Wada, Jpn. J. Appl. Phys., Part 2 **36**, L929 (1997).
[34] A. Ayuela, H. Rabiger, M.J. Puska, and R.M. Nieminen, Phys. Rev. B **66**, 035417 (2002).
[35] N. Zabala, M.J. Puska, H. Raebiger, and R.M. Nieminen, J. Magn. Magn. Mater. **249**, 193 (2002).
[36] A. Krasheninnikov, K. Nordlund, P.O. Lehtinen, A.S. Foster, A. Ayuela, and R.M. Nieminen, Phys. Rev. B **69**, 073402 (2004).
[37] See L. N. Kantorovich, *www.cmmp.ucl.ac.uk/lev*, 2002.